CHAPTER III

SUBCHRONIC EFFECTS OF THE CRUDE EXTRACT FROM *MUCUNA MACROCARPA* ON THE TILAPIA TESTIS

INTRODUCTION

Reproductive effects of the extract from *Mucuna* species on male reproduction are well documented. For example, *M. pruriens* has been used in the traditional medicine for treating male sexual dysfunction. It was found to improve mating behavior, libido and mating potency in male rat (Amin et al., 1996). Whereas, crude extract from *M. urens* at high dose causes complete degeneration of spermatozoa and pyknosis of spermatocytes and spermatids in testicular tubules of male guinea-pigs (Udoh and Ekpenyong, 2001). The black Kwao Krua, *Mucuna macrocarpa* Wall. (synonym: *Mucuna collettii* Lace) has been used in traditional Thai remedy for treatment of male sexual dysfunction. The study on chemical constituents of this plant extract revealed three important compounds including two flavonoids, kaempferol and quercetin, and a stilbenoid, hopeaphenol (Roengsumran et al., 2001). Reproductive effects on male animals were evident among other biological effects of these compounds. Quercetin was found to reduce fertility of male mice (Aravindakshan et al., 1985), inhibit motility of rat spermatozoa due to the inhibition of plasma membrane calcium pump (Nass-Arden and Breitbart, 1990) and inhibit human sperm motility and viability due to decrease in calcium-ATPase activity (Khanduja et al., 2001). Both quercetin and kaempferol also inhibited activity of hyaluronidase in monkey sperm (Li et al., 1997). For hopeaphenol, it is a tetramer of a well known phytoestrogen,

resveratrol. There are two reports on *in vitro* effects of *M. macrocarpa* extract on human tumor cells to determine its antioxidant activity and mutagenicity (Sutjit, 2003) and cytotoxicity (Cherdshewasart, 2004). Reproductive effect of *M. macrocarpa* in form of powder suspension was studied in rat and showed that the 1-month treatment at 10-100 mg/kg had no effect on sex hormone levels and reproductive organs of the adult male rat (Thansa, 2003). However, the reports on biological effects of *M. macrocarpa* crude extract are still limited, especially in toxicological perspective.

Since, the effects of xenobiotics in biological system are not produced unless they and their metabolites reach appropriate sites in the body at a concentration and for a length of time sufficient to produce the effects (Eaton and Klaassen, 2001), reproductive toxicity of xenobiotics is generally assessed in a long-term, low-level experiment. Subchronic toxicity is a toxicity due to chronic exposure to quantities of a toxicant that do not cause any evident acute toxicity for a time period that is extended but is not so long as to constitute a significant part of the lifespan of the species in question (Hodgson and Levi, 2000). One principal goal of the subchronic study is to identify and characterize the specific organ(s) affected by the test compound after repeated administration (Eaton and Klaassen, 2001). In reproductive toxicity study, subchronic assay is thus frequently assigned to assess the effects of chemical in question. To elucidate the plant toxicity on reproductive organ, we used subchronic toxicity bioassay to assess reproductive effects of *M. macrocarpa* crude extract on male Nile tilapia, *Oreochromis niloticus*. Since the reproductive effect can be best identified morphologically at both cellular and subcellular levels using histological methods for light and electron microscopy, changes in testicular structure after exposure to plant extract were determined in the mature tilapia.

MATERIALS AND METHODS

Fish procurement and maintenance

O. niloticus brood stock (3 weeks post-hatching) was obtained from the Aquatic Animal Breeding Research Station at Pathumtani, Department of Fisheries, the Ministry of Agriculture and Cooperatives of Thailand. The fish were raised in 325-L glass aquarium with aerated water. They were maintained on a 14 h light/10 h dark photoperiod at 27-29 °C and fed with commercial fish food (CP Company) twice daily. Water pH ranged between 6.6 and 7.5. The exposure began after fish reached 2 months of age in order to allow complete sex differentiation (Nakamura and Nagahama, 1985; Nakamura et al, 1993; Hines et al., 1999).

Preparation of M. macrocarpa crude extract

Whole stems and tubers of *M. macrocarpa* were ground and dried. The plant powder was extracted with absolute ethanol at room temperature for 2 weeks. Solvent extraction ratio was 1:10, powder (g): solvent (ml). The solution was filtered and the solvent was evaporated out by a rotary evaporator at 40°C at the Natural Products Research Unit, Department of Chemistry, Chulalongkorn University. The crude extract was dried in an oven at 40°C. The extraction process gave approximately 1.51% yield. All crude extracts yielded from each extraction process were pooled together before use in order to minimize variation in chemical composition between each batch.

Subchronic exposure

After the fish reached the age of 2 months, they were separated into 4 aquaria with 300 fish/aquarium. Two aquaria were assigned as the treatment group and the

remaining aquaria were assigned as the control and the solvent control groups. The treatment aquaria were filled with 200 litres of *M. macrocarpa* crude extract solution dissolved in dimethyl sulfoxide (DMSO) at the subchronic concentration of 14 ppm. The control aquarium was filled with 200 litres holding water, and solvent control aquarium was filled with 200 litres of DMSO solution at 20 ppm. The static renewal system was used throughout the experiment, and the holding water of every aquarium was renewed every 4 days. The exposure was carried out continuously for seven months. During the exposure period, fish of every aquarium were sampled (n=20) every month from 4 to 7 months after exposure.

Gonadosomatic index (GSI)

After sampling, the fish were weighed and the testes were removed and weighed. The GSI was calculated as follows:

$$\text{Gonadosomatic index} = \frac{\text{Gonadal weight}}{\text{Body weight}} \times 100$$

The data of gonadosomatic index were collected and analyzed for difference between the control and the treated groups by Student's t-test using SPSS for Windows program (Chicago, IL).

Histology

The testes were fixed in 10% neutral bufferred formalin and processed through standard histological technique for paraffin section (Humason, 1979). All tissue blocks were sectioned at 5 μm and stained with hematoxylin and eosin. Histological structure

and histopathological alterations in the testes were observed by light microscopy (Zeiss Axioskop 40) comparing between the control and the treated groups.

Ultrastructure

Twenty four testes (3 testes from control and 3 testes from treated groups of each sampling month) were sampled and fixed in 4% glutaraldehyde at 4 °C and post-fixed in 2% osmium tetroxide, and then processed through steps in the rapid protocol for TEM processing (Rowden and Lewis, 1974). Semi-thin sections (150-200 nm) were cut with an ultramicrotome (RMC MT-XL), stained with 0.5 % toluidine blue and observed by light microscopy. From 24 semi-thin samples, 8 samples were selected as representatives of every month and processed for thin sections. Thin sections (90-100 nm) were stained with lead citrate and uranyl acetate and were examined with transmission electron microscope (Jeol JEM-2010) at the Department of Biology, Boston University.

RESULTS

Gonadosomatic index

Gonadosomatic indices (GSI) of the control group were 0.19 ± 0.02, 0.15 ± 0.02, 0.15 ± 0.03 and 0.24 ± 0.04 after 4 to 7 months post-exposure. The GSI of the treated group were 0.50 ± 0.13, 0.26 ± 0.06, 0.21 ± 0.05 and 0.22 ± 0.03, respectively. The GSI showed significant differences between the control and the treated groups (Figure 3-1). At 4 and 5 months post-exposure, GSI of the treated fish were significantly higher than that of the control ($p<0.05$). The GSI became similar between groups at 6 and 7 months post-exposure.

Testicular histology

The tilapias (*Oreochromis* sp.) have lobular testes (Le Gac and Loir, 1999) consisting of seminiferous lobules (blind-ended sacs) as germinal compartment. The blind end of each lobule terminates at the tunica albuginea whereas the open end of each lobule terminates at intratesticular collecting duct system. Basic structure of the tilapia lobular testis is shown in Figure 3-2A. The primary spermatogenic unit in fish comprises of an anatomically discrete, closed, spherical compartment termed a spermatogenic cyst or spermatocyst. The spermatocyst contains syncytial germ cell clone embedded in cytoplasm of Sertoli cells, and all germ cells in each spermatocyst are synchronized in development (Callard and Callard, 1999). In *O. niloticus*, each seminiferous lobule comprises of spermatocysts at different spermatogenic stages attached to the seminiferous epithelium in a random fashion (Figure 3-2B-D). Type A spermatogonium can be identified as a large cell with a clear large homogeneous nucleus with one or two nucleolus and each cell is completely surrounded by Sertoli

cells (Figure 3-2B and 3-2E). A clone of type B spermatogonia can be identified as syncytial clone of homogeneous nuclei with small nucleolus (Figure 3-2D-E). A spermatocyte clone can be identified as syncytial clone of smaller heterogeneous nuclei (Figure 3-2B-D). The primary spermatocyte in zygotene stage can be identified at ultrastructural level by synaptonemal complex in nucleus (Figure 3-2E). Because of the duration between first and second meiosis is very short, it is difficult to identify the secondary spermatocyte in fish (Miura, 1999). A spermatid clone can be identified by condensed small nuclei (Figure 3-2B-E). Spermatozoon can be identified as a small condensed nucleus released into the lumen of seminiferous lobule (Figure 3-2C). Degeneration of an entire spermatocyst can be observed in some lobules of normal testis as a cluster of apoptotic bodies (Figure 3-2E). Interlobular space of testis was resided by clusters of Leydig cells, blood capillaries and fibroblasts (Figure 3-2B-C).

Testicular histopathological alterations

Testicular tissues of the control and solvent control tilapias were normal at every month examined. Hence, the results observed from these 2 control groups are collectively presented as 'the control' in this study. The control testes contained seminiferous lobules with spermatocysts at different stages of development (Figure 3-3E, 3-4C, 3-7C and 3-8E). All testes of the control fish at 4 to 7 months post-exposre, regardless of its size, showed seminiferous lobules with thick, healthy spermatocysts at different stages of development, including spermatozoa in the lumens. Some apoptosis of germ cells were found after 5 months post-exposure as a cyst of numerous apoptotic bodies. At 6 months post-exposure, some testes possessed seminiferous lobules with only the early-stage spermatocysts and the efferent ducts contained a mass of

homogeneous eosinophilic material. At 7 months post-exposure, almost all testes had seminiferous lobules with thick, healthy spermatocysts at different stages and spermatozoa in the lumens.

In the treated fish at 4 months post-exposure, degenerations of spermatocysts were found (Figure 3-3F and 3-4D). Some seminiferous lobules collapsed (Figure 3-4B and 3-4D). There was an extensive loss of testicular tissue (Figure 3-3C-D). Infiltrations of eosinophils and macrophages were also found in the tunica albuginea and in the interlobular spaces (Figure 3-4E-F). Apoptosis was found in 57% of individuals observed. At 5 months post-exposure, high proliferations of Leydig cells were found in both control and treated groups (Figure 3-5C-D). In the treated fish, degenerations of spermatocysts were also observed with abundant apoptotic bodies in the seminiferous lobules (Figure 3-5E-F). The apoptosis found in the testes at this period was more severe even though it occurred in only 40% of individuals observed. At 6 months post-exposure, high proliferations of Leydig cells were also found in both control and treated groups (Figure 3-6C-F). The treated testes showed seminiferous lobules with larger lumen size and thicker epithelium compared with that of the controls (Figure 3-6D-E). Infiltrations of macrophages in the interlobular spaces were observed (Figure 3-6E). Degenerations of spermatocysts with numerous apoptotic bodies were also found (Figure 3-6F). In the treated fish at 7 months post-exposure, abnormal testicular tissue with large ductal area was found (Figure 3-7B). The efferent duct was found to contain a few spermatozoa (Figure 3-7D). Degenerations of spermatocysts with large vacuoles were also observed (Figure 3-7F).

Complete spermatogenesis is evidenced by observation of spermatozoa in the seminiferous lumens. In the control fish, spermatogenesis was complete in all

individuals observed since 4 months post-exposure, whereas only 57% of the treated fish in this month possessed complete spermatogenesis. Complete spermatogenesis in all treated fish was observed after 6 months post-exposure.

Proliferation of Leydig cells was observed in some individuals in both control and treated fish, except at 4 months post exposure that there was no clear evidence of Leydig cell proliferation in the treated fish. Leydig cells were highly proliferated after 5 months post-exposure in both control and treated fish. All treated fish observed at this period possess testes with high proliferation of Leydig cells. The proliferation then declined at 7 months post-exposure in both groups.

Ultrastructural changes during spermatogenesis

Germ cells in seminiferous lobules of the tilapia undergo cytodifferentiation during spermatogenesis. Identification of germ cell stages during spermatogenesis in *O. niloticus* presented in this study is based on Miura (1999) and the study in cichlid fish by Fishelson (2003). Ultrastructural study revealed different germ cell stages in the seminiferous lobule of *O. niloticus* testis consisting of type A spermatogonium, type B spermatogonium, spermatocyte and spermatid. Each stage of germ cells was surrounded by Sertoli cells forming a primary spermatogenic unit, spermatocyst.

Type A spermatogonium. Large germ cell (5-7 μm) possesses a large homogeneous nucleus with one large nucleolus. Nuclear membrane has several indentations with electron-dense nuclear bodies in the grooves at cytoplasmic side. Each type A spermatogonium is completely surrounded by Sertoli cells (Figure 3-8A-B).

Type B spermatogonium. Germ cell possesses a spherical nucleus with small nucleolus. Cytoplasm contains mitochondria with electron-dense matrix. Type B

spermatogonia proliferate by mitosis and appear as a syncytial clone surrounded by Sertoli cells (Figure 3-8C).

Spermatocyte. Primary spermatocyte entering the first meiotic prophase is identified at the zygotene stage by the presence of synaptonemal complex, a complex of pairing sister chromatids (Figure 3-10D). Nuclear membrane is partially disappeared. Cytoplasm contains mitochondria with electron-dense matrix (Figure 3-8D).

Spermatids. Small haploid germ cells undergo spermiogenesis and progress into several stages. There are remarkable ultrastructural changes involved the formation of head, midpiece and flagellum. In this study, we identified 4 stages of spermatids including spermatid I, spermatid II, spermatid III and spermatid IV. Spermatid I possesses small spherical heterogeneous nucleus and condensed cytoplasm with mitochondria with electron-dense matrix (Figure 3-8E). The spermatids in the same spermatocyst are connected by wide cytoplasmic bridges. Spermatid II possesses small electron-dense homogeneous nucleus and also condensed cytoplasm with electron-dense mitochondria (Figure 3-8E). The nucleus has a deep indentation (fossa) in which two centrioles reside. The spermatids are still connected by cytoplasmic bridges. The formation of flagellum is not observed in these two stages. Spermatid III possesses nucleus with dispersed dark chromosomal bodies as the head (Figure 3-9A). Microtubules of developing flagella are seen. Mitochondria are found in the midpiece called cytoplasmic collar. Spermatid IV possesses the head containing condensed and aggregated dark chromosomal bodies (Figure 3-9B). Mitochondria are packed in the cytoplasmic collar. Flagellum with its microtubules is observed.

Ultrastructure of germ cells during spermatogenesis in the treated tilapia was not different from the control when compared at stage by stage. The structures of type A

spermatogonium, type B spermatogonium and spermatocyte at zygotene stage of meiosis are shown in Figure 3-10 and spermatid I, spermatid III and spermatid IV are shown in Figure 3-11A-B. Degenerations of germ cells were observed in both control and treated tilapia. All germ cells in the same spermatocyst were dead and observed as apoptotic bodies surrounded by Sertoli cells (Figure 3-9C and 3-11C).

DISCUSSION

In this study, histological and ultrastructural endpoints were used to assess potential reproductive effects of *M. macrocarpa* crude extract on the male tilapia. Testicular development based on gonadosomatic index showed significant differences in the early exposure period. The GSI of the treated fish were significantly higher than that of the control ($p<0.05$) at 4 and 5 months post-exposure and then became similar between groups at 6 and 7 months post-exposure.

As the GSI is an indicator of the reproductive health in animal, different GSI between treatments is usually linked to different gonadal development due to reproductive effects of the test chemicals. Similar to the present study, the temporary increase in male GSI has been reported in small fish species collected from endocrine disrupting chemicals (EDCs)-polluted sites in Athabasca oil sand area, Canada (Tetreault et al., 2003). An aromatase inhibitor, fadrozole (at 51.7 and 95.5 μg/l), has also been reported to significantly induce testicular growth and higher GSI in pre-spawning adult fathead minnows (*Pimephales promelus*) (Panter et al., 2004). But injection of fadrozole (1.0-10.0 mg/kg) in maturing coho salmon (*Oncorhynchus kisutch*) did not affect the male GSI (Afonso et al., 2000). On the contrary, studies on effects of estrogenic chemicals on male fish revealed that the major effect was the inhibition of testicular growth with significant reduction of GSI (Condeça and Canario, 1999; Mills et al., 2001; Rasmussen and Korsgaard, 2004; Brion et al., 2004). However, in some studies, long-term exposure to low concentration of estrogen caused no significant difference of GSI between groups in mature medaka, *Oryzias latipes* (Scholz and Gutzeit, 2000). The studies of the effects of some other endocrine disrupting chemicals (EDCs) on fish GSI also gave similar results. Long-term treatments with combinations

of testosterone, gonadotropin-releasing hormone agonist and pimozide (dopamine antagonist) resulted in a reduction of male GSI in maturing striped bass, *Morone saxatilis* (Holland et al., 2002). Whereas, treatment of anti-androgenic chemical, *p,p'*-DDE, in juvenile summer flounder, *Paralichthys dentatus*, did not alter the male GSI (Mills et al., 2001).

From histological results, all testes of the control fish undergo complete spermatogenesis at earlier period than the treated fish. A minor exception was found at 6 months post-exposure when complete spermatogenesis was seen in some individuals, while the other possessed seminiferous lobules containing only spermatocysts in early stages with some apoptotic cysts and homogeneous eosinophilic material in the lumens which may indicate post-spermiation phase. However, complete spermatogenesis was observed in all control fish again at 7 months post-exposure. The GSI of the control fish was relatively unvarying, ranging from 0.15 to 0.24. The period of high GSI correlated well with the occurrence of complete spermatogenesis. In contrast, this correlation was not applied to the treated testis. The highest GSI of the treated fish (0.50) at 4 months post-exposure was not associated with the complete spermatogenesis. Whereas, the complete spermatogenesis was first observed in the treated group at 6 months post-exposure, when the GSI was at the lowest value (0.21). The GSI change in the treated fish may be the result of histopathological alterations rather than the enhanced testicular development. Thus, based on the results of this study, GSI should not be used as a sole indicator for reproductive toxicity assessment in male fish since high GSI may also be due to histopathological alterations, not the gonadal maturity. It is of importance to note the overall result suggesting that spermatogenesis in the treated fish is not altered, but may be delayed due to the exposure to the plant extract.

Evidences of degenerative stage of testis (post-spermiation phase) were observed in both control and treated fish around 6 to 7 months post-exposure, and were not described as the histopathological change in this study. In contrast, the 8-week treatment of crude extract from *M. urens* at 140 mg/kg in mature guinea-pigs was reported to cause complete degeneration of sperm in the testicular tubules, pyknosis of spermatocytes and spermatids whereas spermatogonia are still normal (Udoh and Ekpenyong, 2001).

Alteration of testicular structure found in this study may be associated with the hormonally active ingredients found in the *M. macrocarpa* extract. Hopeaphenol is a tetramer of resveratrol, an agonist for the estrogen receptor (Gehm et al., 1997). Quercetin and kaempferol show a weak anti-estrogenic activity (Papiez et al., 2002). In the studies of reproductive effects from long-term treatment of estrogenic chemicals on male fish, high concentration of estrogen generally induces intersex (testis-ova) males or sex-reversed females, and low concentration of estrogen may produce no effect or may inhibit/regress testicular growth and germ cell development. In long-term treatment of 17α-ethinylestradiol to male medaka, *Oryzias latipes*, from early-life stage, 10 ng/l treatment produced almost 70% sex-reversed females (Balch et al., 2004) and 100 ng/l treatment produced 100% sex-reversed females (Scholz and Gutzeit, 2000). However, there was no evidence of intersex or sex-reversed tilapia in the current study.

Long-term treatment of estradiol-17β to adult male sea bream, *Sparus aurata*, at 2-15 mg/kg inhibited testicular growth and arrested germ cell development beyond the spermatogonia stage (Condeça and Canario, 1999). In the treatments of several estrogenic chemicals (flutamide, *p,p'*-DDE, 4-*tert*-octylphenol and bisphenol A) to mature guppy, *Poecilia reticulata*, they caused similar effects including a reduction in

number of spermatocysts but there was an increase in number of spermatozeugmata in the ducts (Kinnberg and Toft, 2003). The treatment of octylphenol (100 mg/kg) in juvenile summer flounder, *Paralichthys dentatus*, caused reduction of testicular size with numerous spermatogonia, no developing spermatocyst and the ducts full of spermatozoa in the early treatment period and then the testes were developed similar to the control in the later period (Zaroogian et al., 2001). These two studies show that spermatogenesis of the treated fish is still complete. It implies that low-concentration treatment of estrogenic chemicals in adult male fish may temporarily alter the spermatogenesis.

An interesting histopathological alteration occurred in this study is an increase of germ cell apoptosis in the treated fish. Testicular apoptosis accounts for the reduction in number of germ cells during mitotic divisions of spermatogonia, meiosis of spermatocytes and spermiogenesis (Terranova and Taylor, 1999). It naturally occurs in fish testis in all-or-none fashion that all germ cells in a spermatocyst are degenerated (Callard and Callard, 1999). In the control fish, a few apoptotic nuclei occurred in some testes after 5 months post-exposure. In the treated fish, apoptosis was found between 4 to 6 months post-exposure. High degree of apoptosis (numerous apoptotic spermatocysts in a testis) was observed in the treated testes at 5 and 6 months post-exposure. Induction of germ cell apoptosis in the fish exposed to the plant extract may involve with the activity of quercetin, one of the chemical compounds found in *M. macrocarpa* extract. This constituent of the black Kwao Krua has been reported to increase DNA fragmentation and caspase-3 activity in HPB-ALL cell line (Russo et al., 1999), enhance apoptotic DNA fragmentation in HL-60 and L1210 cell lines (Iwao and

Tsukamoto, 1999), and inhibit DNA synthesis and induce apoptosis in regenerating liver after partial hepatectomy (Čipák et al., 2003).

Overall, the present study examined the effects of *M. macrocarpa*, a plant used in traditional remedy for treating male sexual dysfunction and containing several hormonally active ingredients. The results from subchronic treatment on male tilapia show no indication of an enhanced reproductive effect of this plant extract. But there were some pathological alterations of testicular tissues in the fish exposed to the plant extract. Although the spermatogenesis was comparatively delayed, it was not entirely inhibited. The ultrastructure of germ cells in the testis that were capable of complete spermatogenesis was not altered from the treatment of the plant extract. It is of interest to further examine the effect of this plant extract on structure of female reproductive system, as well as examine the effect on the steroidogenic function of fish gonad.

FIGURES

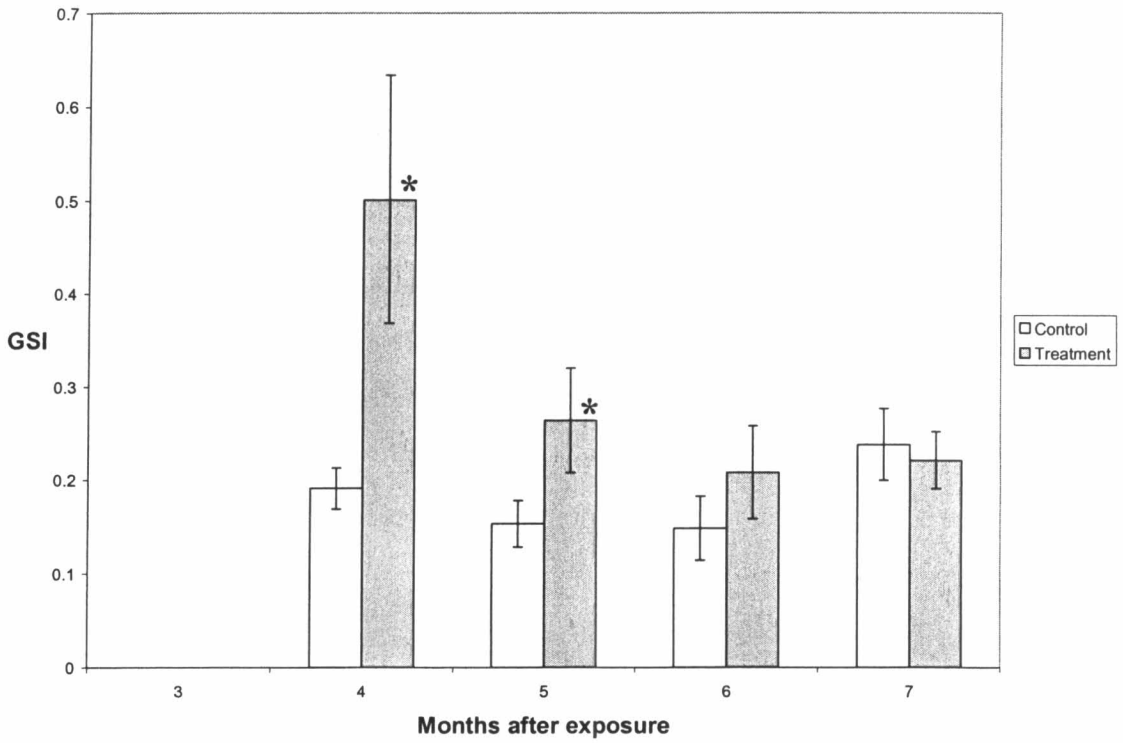

Figure 3-1: Gonadosomatic indices (GSI) of the male tilapia after 4 to 7 months of exposure (mean ± SE). * Indicates significant differences from respective controls ($p < 0.05$).

Figure 3-2: Basic histological structure of the tilapia *O. niloticus* testis. (A) Illustration of the lobular testis. (B-D) Seminiferous lobule consists of spermatocysts at each stage lining the seminiferous epithelium (white arrows). Cluster of Leydig cells is seen in the interlobular space (*). *Bar*: 20 μm. *Toluidine blue stain*. (E) Electron micrograph of spermatocysts in the seminiferous lobule. Degenerated spermatocyst containing apoptotic bodies is noted (yellow circle). *Bar*: 2 μm.

SgA type A spermatogonium, *SgB* type B spermatogonium, *Sc* spermatocyte, *St* spermatid, *Sm* spermatozoon, *Se* Sertoli cell.

Figure 3-2

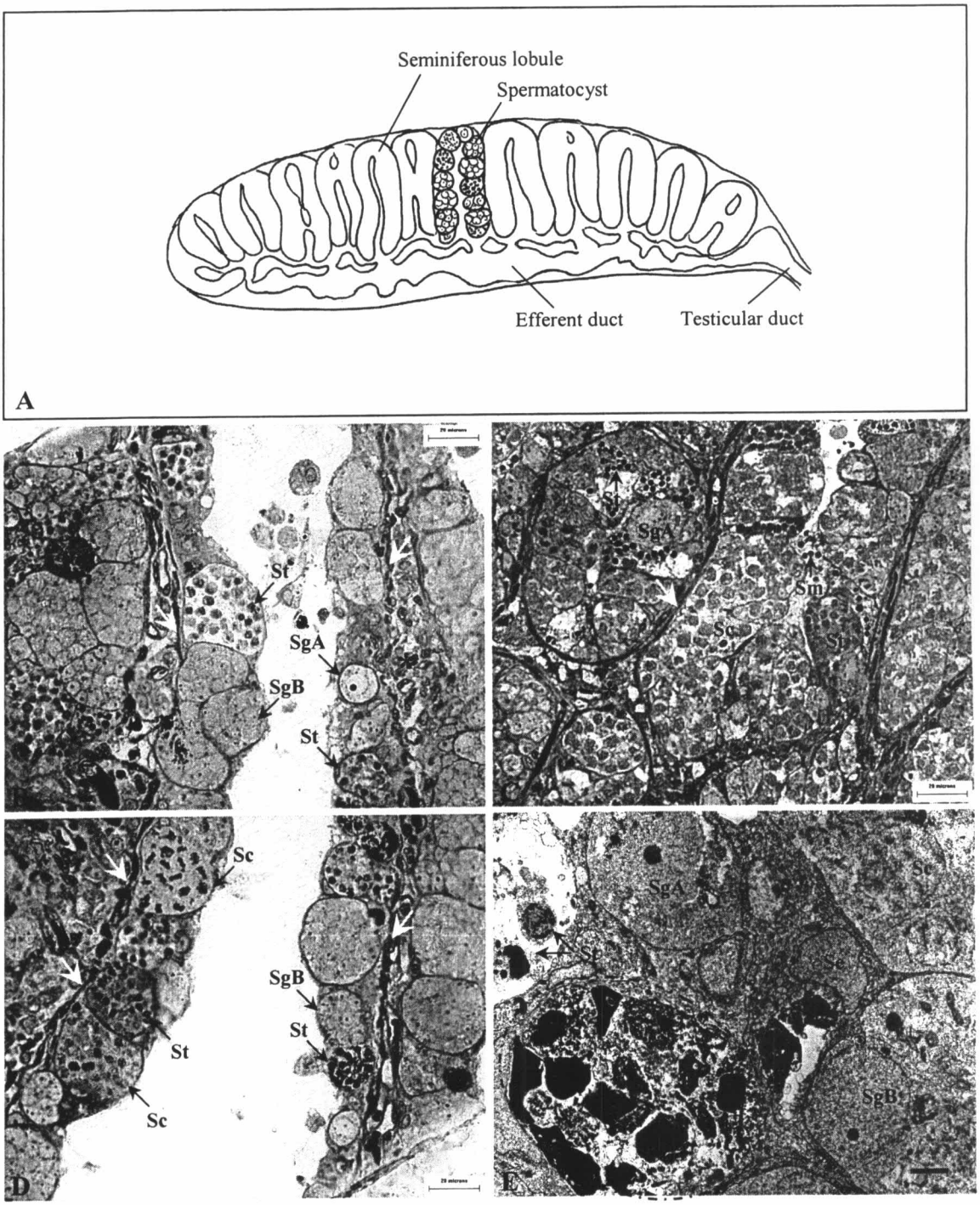
Seminiferous lobule
Spermatocyst
Efferent duct
Testicular duct
A
St
SgA
SgB
St
Sc
St
SgA
Sm
Sc
Sp
Sc
SgB
St
St
Sc
SgA
Sc
Sp
SgB
D
E

Figure 3-3: Testes of *O. niloticus* at 4 months post-exposure. (A-B) Longitudinal section of testis of the control fish shows normal histological structure. *Bar*: 150 μm. (C-D) Longitudinal section of testis of the treated fish shows extensive loss of testicular tissue (*). *Bar*: 150 μm. (E) High magnification of the control testis shows seminiferous lobules with spermatocysts at different stages compared with the treated testis (F) with degenerated spermatocysts. *Bar*: 20 μm. *H&E stain*.

Figure 3-3

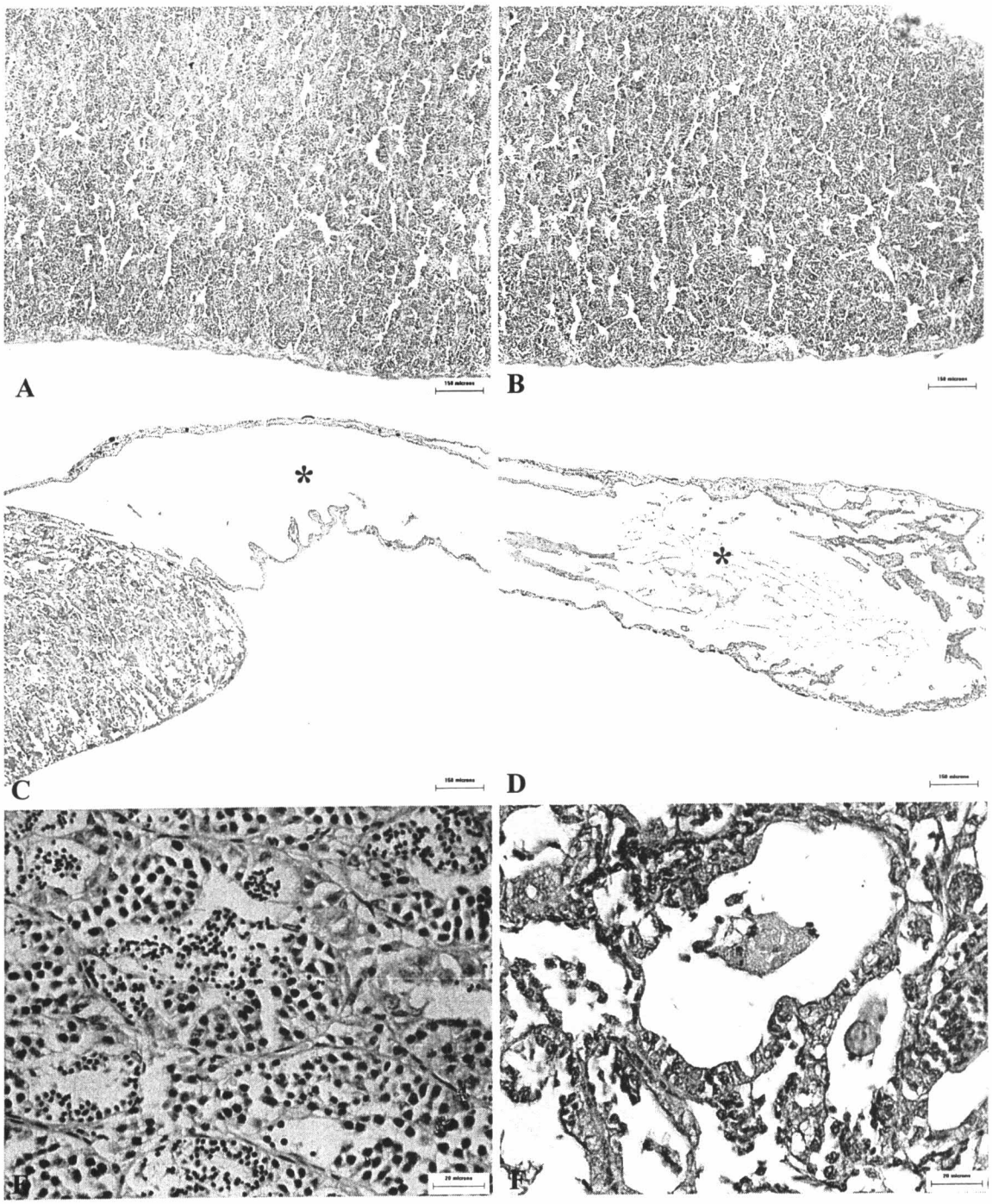

Figure 3-4: Testes of *O. niloticus* at 4 months post-exposure. (A) Normal testicular tissue of the control fish. *Bar*: 80 μm. (B) Testis of the treated fish shows degeneration of spermatocysts in several lobules. *Bar*: 80 μm. (C) Normal spermatocyst (*) with thin connective tissue bounded contains synchronized germ cells. *Bar*: 20 μm. (D) Collapse of spermatogenic lobules in the treated testis. Degenerated spermatocysts (*) are noted. *Bar*: 20 μm. (E) Infiltration of macrophages (arrow) in testicular capsule of the treated fish. *Bar*: 80 μm. (F) Infiltration of macrophage (arrow) in interlobular area of the treated testis. Inset shows penetration of eosinophils and macrophages (arrow) through the endothelium of testicular blood vessel (Bv). *Bar*: 20 μm. *H&E stain*.

Figure 3-4

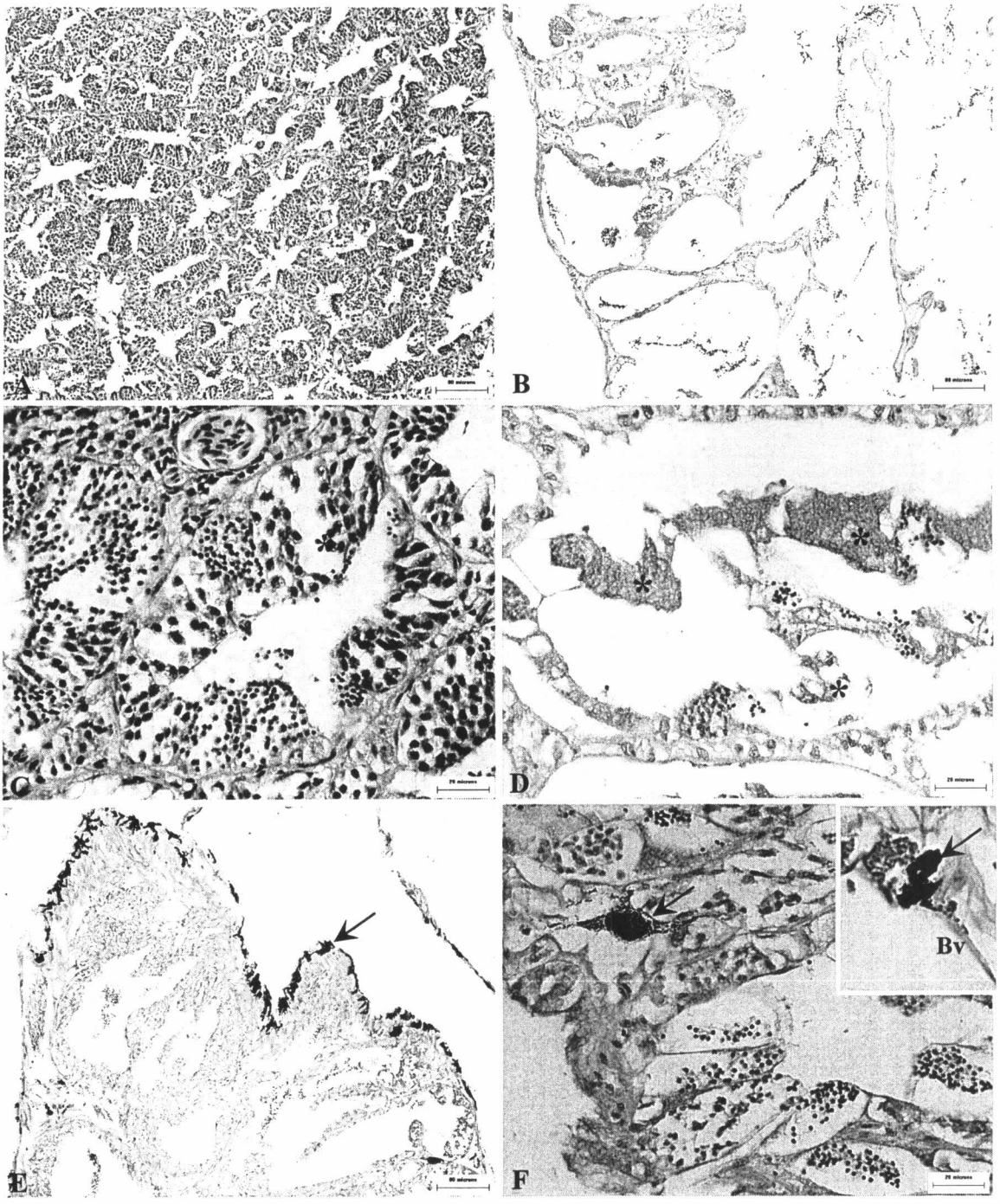

Figure 3-5: Testes of *O. niloticus* at 5 months post-exposure. (A) Normal testicular tissue of the control fish. *Bar*: 150 μm. (B) Testicular tissue of the treated fish with complete spermatogenesis. Abundant spermatozoa in efferent duct are seen (∗). *Bar*: 150 μm. (C) Proliferation of Leydig cells (∗) in the control testis. *Bar*: 20 μm. (D) Proliferation of Leydig cells (∗) in the treated testis. *Bar*: 20 μm. (E) High degree of apoptosis (arrows) in the treated testis. *Bar*: 40 μm. (F) Apoptotic bodies (arrows) and degenerated spermatocyst (∗) in the treated testis. *Bar*: 20 μm. *H&E stain*.

C capillary.

Figure 3-5

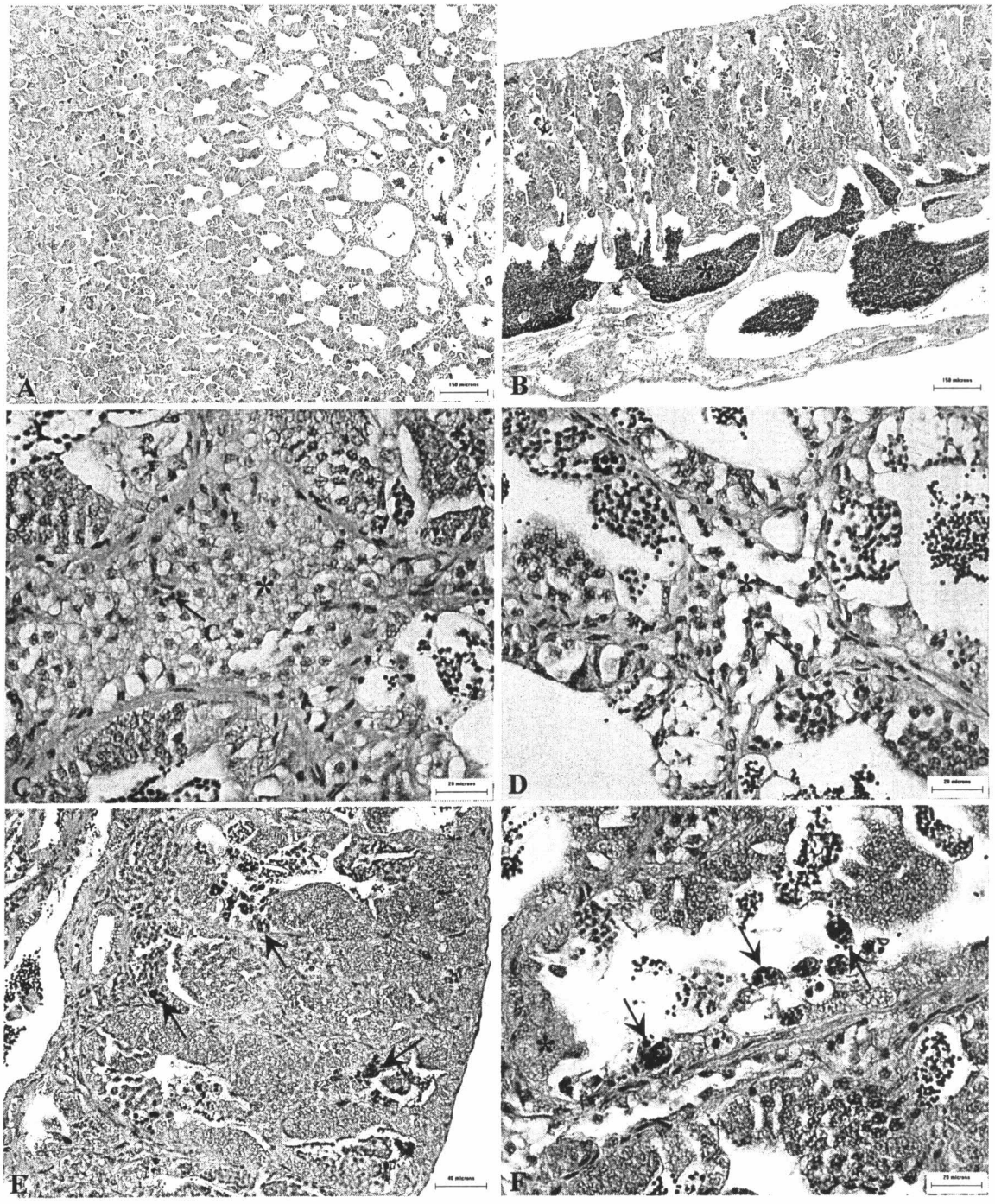

Figure 3-6: Testes of *O. niloticus* at 6 months post-exposure. (A) Normal testicular tissue of the control fish with complete spermatogenesis. *Bar*: 150 μm. (B) Testicular tissue of the treated fish with complete spermatogenesis. *Bar*: 150 μm. (C) Control testis shows Leydig cell proliferation (*). *Bar*: 20 μm. (D) Treated testis shows seminiferous lobule with large lumen filled with spermatozoa and Leydig cell proliferation (*). *Bar*: 20 μm. (E) Treated testis with thick seminiferous epithelium (arrowheads) and infiltration of macrophages (arrows). *Bar*: 40 μm. (F) Treated testis shows degeneration of spermatocysts with apoptotic bodies (arrows). Proliferation of Leydig cells is also noted (*). *Bar*: 20 μm. *H&E stain*.

Figure 3-6

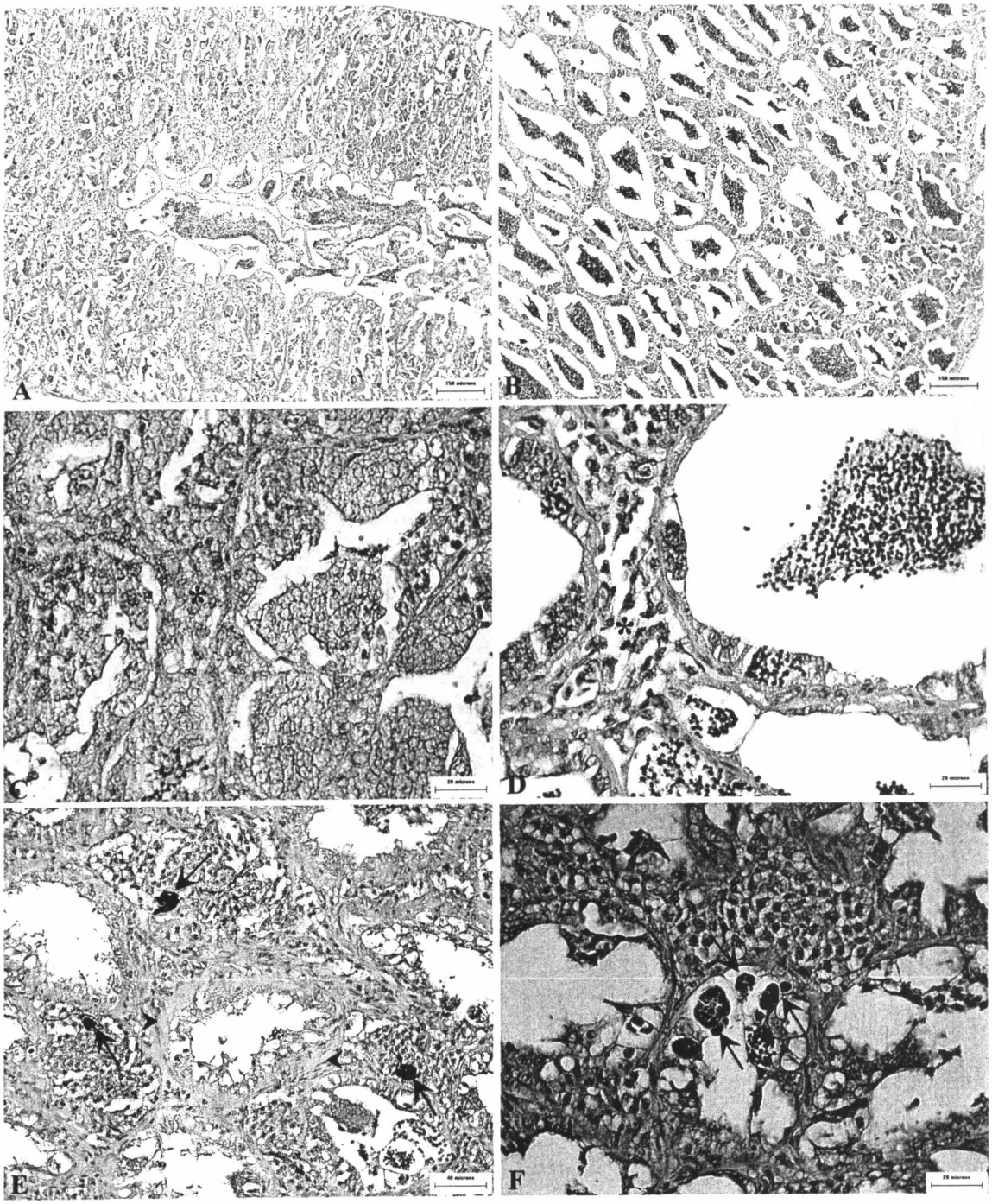

Figure 3-7: Testes of *O. niloticus* at 7 months post-exposure. (A) Normal testicular tissue of the control fish with complete spermatogenesis. *Bar*: 150 μm. (B) Abnormal testicular tissue of the treated fish with large ductal area (*). *Bar*: 150 μm. (C) Efferent duct of the control testis contains abundant spermatozoa. *Bar*: 40 μm. (D) Efferent duct of the treated testis contains a few spermatozoa. *Bar*: 40 μm. (E) Seminiferous lobule of the control testis with different stages of spermatocysts and spermatozoa in the lumen. *Bar*: 20 μm. (F) Seminiferous lobules of the treated testis contain degenerated spermatocysts with large vacuoles (arrows). *Bar*: 20 μm. *H&E stain*.

Figure 3-7

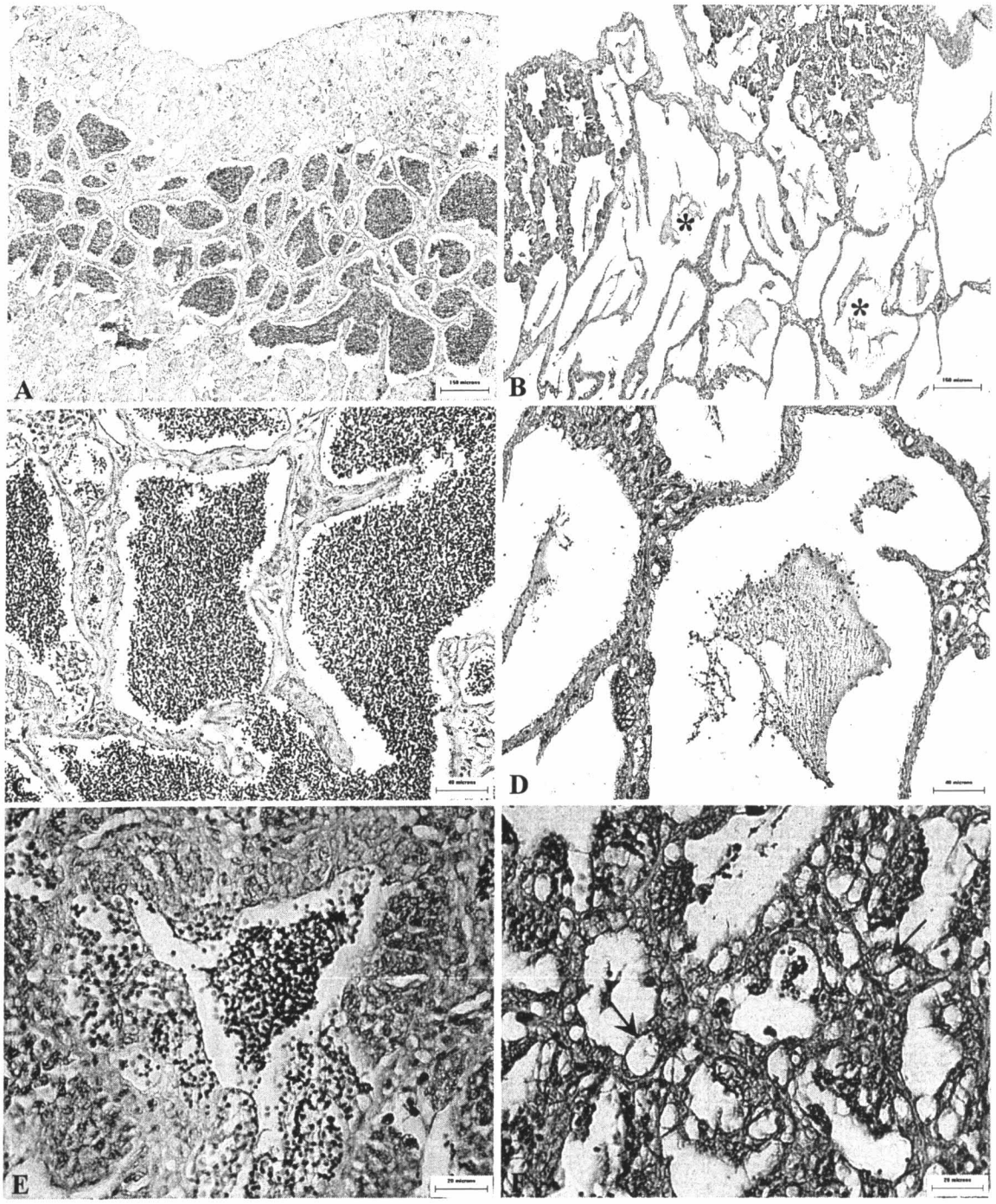

Figure 3-8: Electron micrograph of the control *O. niloticus* testes. (A) Type A spermatogonium with a large nucleolus and dense nuclear bodies (arrow) outside the nucleus. ×5,000. *Bar*: 1 μm. (B) Dividing type A spermatogonia. Dense nuclear bodies (arrow) are still visible. ×5,000. *Bar*: 1 μm. (C) Type B spermatogonia with spherical nucleus and small nucleolus. ×3,000. *Bar*: 2 μm. (D) Spermatocytes at zygotene stage of meiosis. The synaptonemal complex in nucleus is indicated by an arrow. ×3,000. *Bar*: 2 μm. (E) Early spermatid at stage I with spherical heterogeneous nucleus and condensed cytoplasm and spermatid II with small homogeneous nucleus, deep fossa with two centrioles (arrowheads) and bridge between spermatids (arrow). ×3,000. *Bar*: 2 μm.

SgA type A spermatogonium, *SgB* type B spermatogonium, *Sc* spermatocyte, *StI* spermatid I, *StII* spermatid II, *Se* Sertoli cell.

Figure 3-8

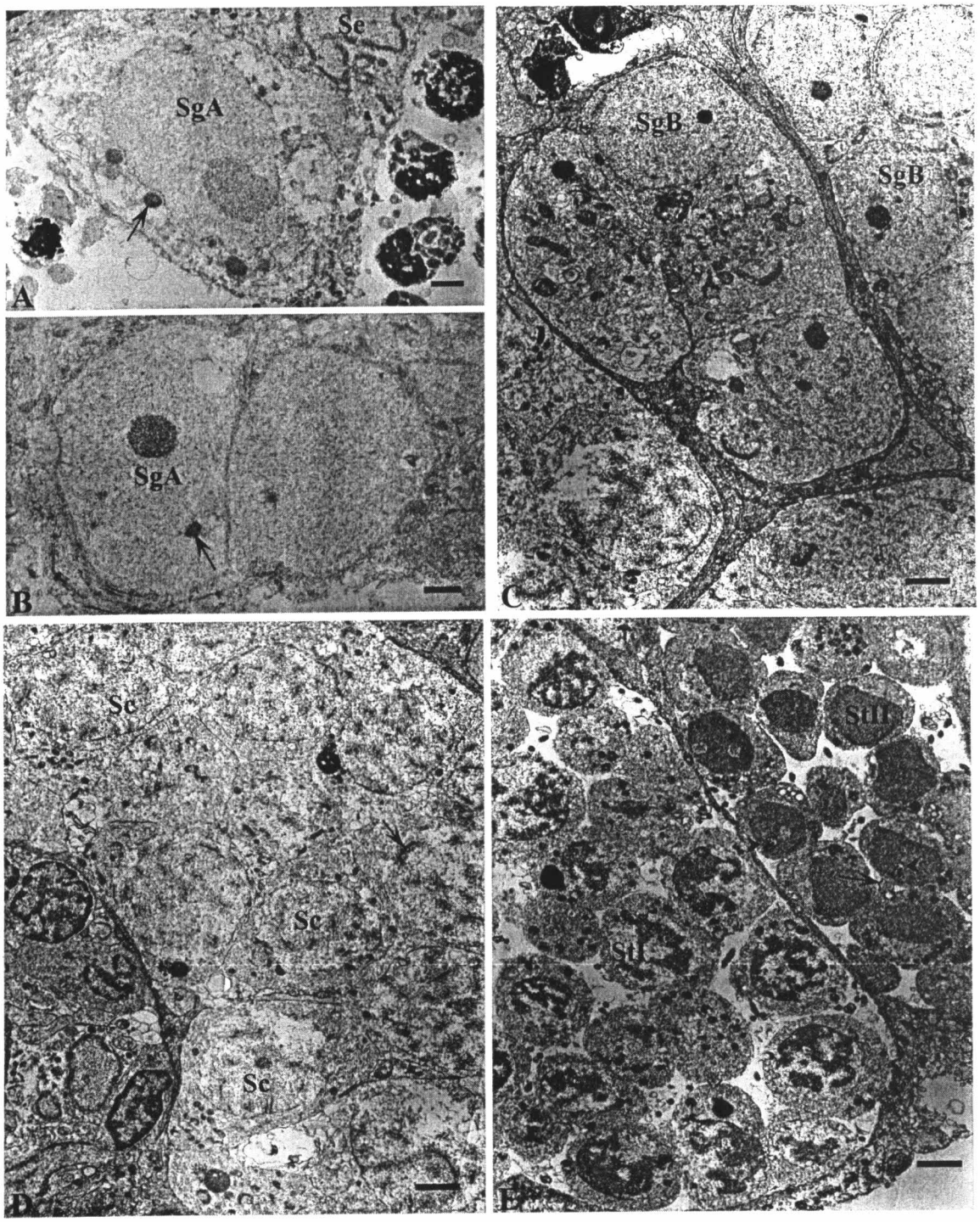

Figure 3-9: Electron micrograph of the control *O. niloticus* testes. (A) Spermatid at stage III with dispersed dark chromosomal bodies (arrow) and microtubules of developing flagellum (arrowhead). ×4,000. *Bar*: 2 μm. (B) Late spermatid at stage IV with aggregated dark chromosomal bodies at the heads. Cross sections of flagellum (arrows) and mitochondria (arrowheads) packed in the cytoplasmic collar are seen. ×6,000. *Bar*: 1 μm. (C) Spermatocysts at different stages surrounded by the Sertoli cells. Cysts of degenerative germ cells (*) are noted. ×3,000. *Bar*: 2 μm.

SgA type A spermatogonium, *SgB* type B spermatogonium, *Sc* spermatocyte, *StIII* spermatid III, *StIV* spermatid IV, *Se* Sertoli cell.

Figure 3-9

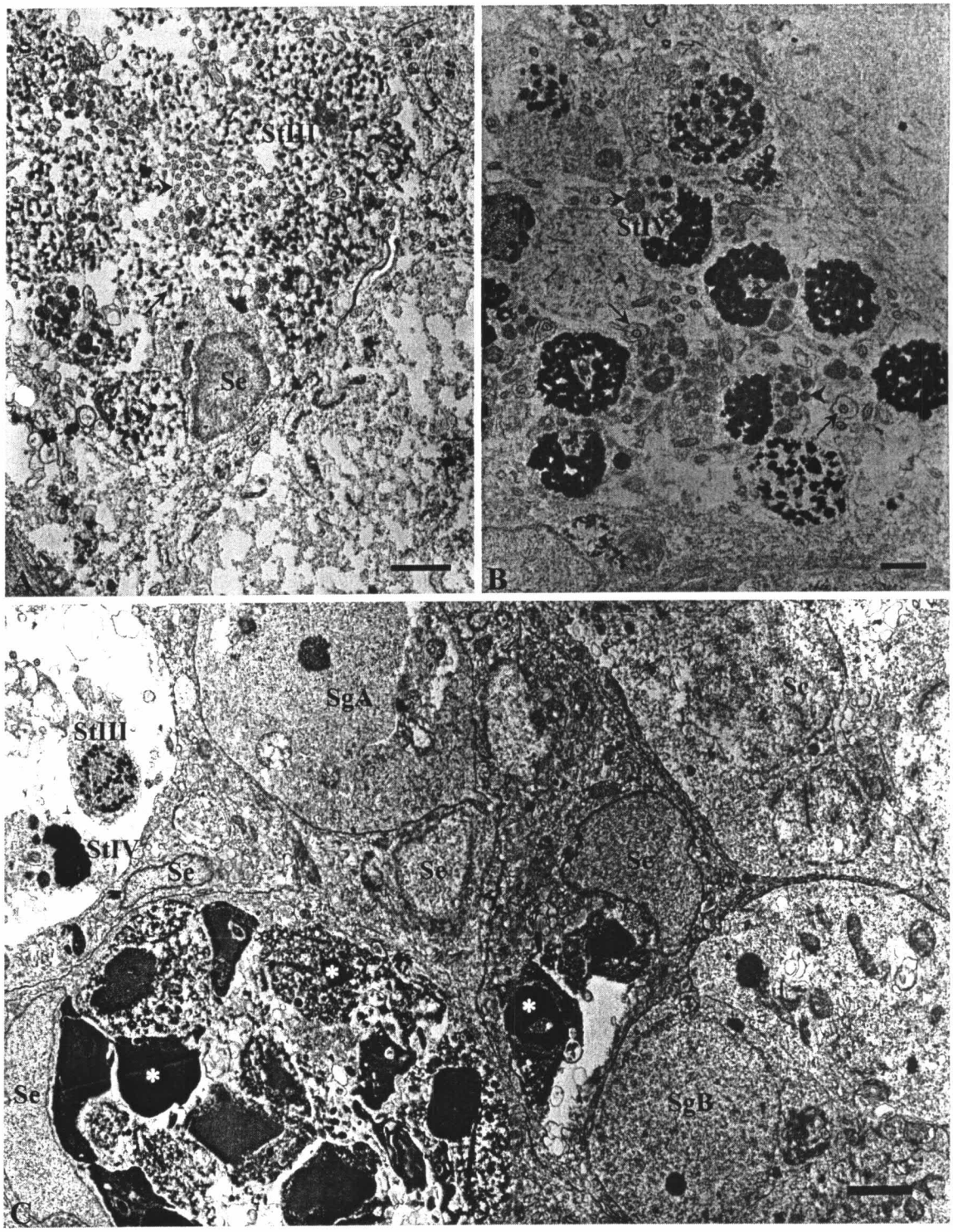

Figure 3-10: Electron micrograph of the treated *O. niloticus* testes. (A) Type A spermatogonium with a large nucleolus and dense nuclear bodies (arrow) outside the nucleus. ×3,000. *Bar*: 2 μm. (B) Type B spermatogonia with spherical nucleus and small nucleolus. ×5,000. *Bar*: 1 μm. (C) Spermatocytes at zygotene stage of meiosis with synaptonemal complex (arrow). ×5,000. *Bar*: 1 μm. (D) Zygotene spermatocyte with electron-dense mitochondria and synaptonemal complexes showing union of the sister chromatids (arrows). ×12,000. *Bar*: 500 nm.

SgA type A spermatogonium, *SgB* type B spermatogonium, *Sc* spermatocyte, *Se* Sertoli cell, *m* mitochondria.

Figure 3-10

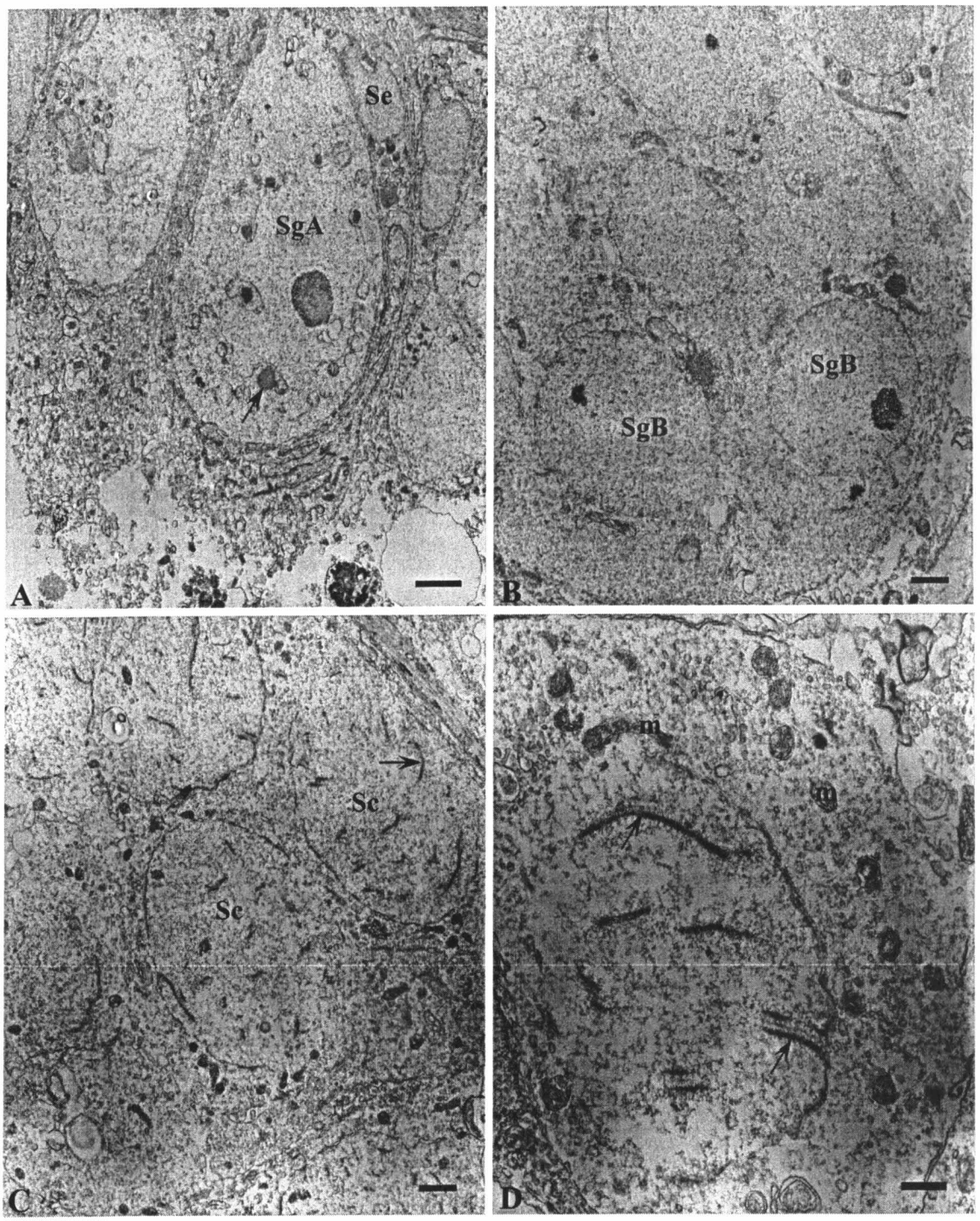

Figure 3-11: Electron micrograph of the treated *O. niloticus* testes. (A) Spermatid I with spherical heterogeneous nucleus and condensed cytoplasm. ×3,000. *Bar*: 2 μm. (B) Spermatid III with some dispersed dark chromosomal bodies and spermatid IV with flagellum (arrows) and mitochondria (arrowheads) packed in the cytoplasmic collar. ×5,000. *Bar*: 1 μm. (C) Cysts of degenerative germ cells (*), one is engulfed by Sertoli cell. ×3,000. *Bar*: 2 μm.

StI spermatid I, *StIII* spermatid III, *StIV* spermatid IV, *Se* Sertoli cell, *E* erythrocyte .

Figure 3-11